Including charge penetration effects into the ESP derived partial charge operator

AUTHOR(S):

Nakano, Hiroshi; Yamamoto, Takeshi

CITATION:

Nakano, Hiroshi ...[et al]. Including charge penetration effects into the ESP derived partial charge operator. Chemical Physics Letters 2012, 546(12): 80-85

ISSUE DATE:

2012-09

URL:

http://hdl.handle.net/2433/160033

Including charge penetration effects into the ESP derived partial charge operator

Hiroshi Nakano and Takeshi Yamamoto*

Department of Chemistry, Graduate School of Science,

Kyoto University, Kyoto 606-8502, Japan

Abstract

Electrostatic potential (ESP) derived partial charge provides a useful tool for describing intermolecular electrostatic (ES) interactions. One can also devise a corresponding charge "operator" that generates partial charge upon taking the expectation value over molecular wavefunctions. While the ESP charge operator has been utilized in various QM/MM(-type) calculations, it has the drawback that short-range ES interactions are overestimated due to the neglect of charge penetration effects. Here, we develop a screened version of the ESP charge operator that includes penetration effects at short range and thereby improve its accuracy. Numerical tests are performed for typical ions in aqueous solution.

*Electronic address: yamamoto@kuchem.kyoto-u.ac.jp

I. INTRODUCTION

The utility of molecular dynamics (MD) simulation heavily relies on an accurate description of intermolecular interactions. In classical MD simulation, it is common to employ a force field expressed in terms of atom-centered interaction sites. Electrostatic (ES) interactions are usually represented by a set of point charges or point dipoles, with their parameters determined from ab initio ESP fitting calculation. The ESP derived charge or dipole thus obtained, however, has the well-known drawback that it becomes less accurate at short range due to the neglect of charge penetration effects (i.e., the overlap of molecular charge distribution). As such, theoretical efforts have been continued to obtain more accurate models for molecular interactions by explicitly including charge penetration effects at short range [1–5].

The limited accuracy of ESP derived charge is also pertinent to the ESP derived partial charge "operator" [6–9]. The latter is defined such that it generates partial charge upon taking the expectation value over a molecular wave function, i.e. $Q_a = \langle\Psi|\hat{Q}_a|\Psi\rangle$. The benefit of using such an operator is that one can recast the quantum mechanical/molecular mechanical (QM/MM) interactions into the form of an interaction site model. This in turn facilitates the development of electronic structure theory combined with other classical theories for the environment (e.g., integral equation theory for solvent). As such, the ESP charge operator has been utilized previously in the development of reference interaction site model self-consistent field (RISM-SCF) method [8–10], charge response kernel (CRK) for electronic polarization [6, 7, 11], QM/MM(-type) calculations [12–17], and nonequilibrium solvation theory for chemical reactions [18, 19]. It is also noteworthy that a more general form of ESP derived multipole operator has been developed [20] and applied to various systems [21–23]. A significant benefit of such an operator is that it can account for a large number of MM point charges (say, $> 10^6$) at negligible computational costs, while allowing a straightforward treatment of QM-MM interactions under periodic boundary condition.

Despite these benefits, the ESP derived charge operator $\hat{Q}_a$ has the drawback that short-range ES interactions are overestimated due to the neglect of penetration effects. Therefore, our purpose in this paper is to explore a way to improve the accuracy of the ESP charge operator by explicitly considering charge penetration effects at short range (Sec. II). We note that a similar problem has been addressed previously, e.g., by the RISM-SCF spatial electron

density distribution (SEDD) method [24]. In the latter method, the charge density of the solute molecule is expanded in terms of Gaussian basis functions, and an effective interaction operator is constructed based on the Gaussian density fitting. On the other hand, the present study aims at obtaining a simple modification of the existing ESP charge operator by considering screening effects of valence electrons and obtaining necessary parameters from ab initio ESP calculation. Test calculations show that the screened charge operator significantly improves upon the original ESP charge operator for typical ions in aqueous solution (Sec. IV).

II. THEORY

In the usual QM/MM calculation, one solves the following equation for the QM molecule

$$[\hat{H}_0 + \int d\mathbf{x}\hat{\rho}(\mathbf{x})v(\mathbf{x})]|\Psi\rangle = \mathcal{E}|\Psi\rangle, \tag{1}$$

where $\hat{H}_0$ is the QM Hamiltonian in the gas phase, $\hat{\rho}(\mathbf{x})$ is the charge density operator given by

$$\hat{\rho}(\mathbf{x}) = \sum_a^{\text{nuc}} Z_a\delta(\mathbf{x} - \mathbf{R}_a) - \sum_i^{\text{ele}} \delta(\mathbf{x} - \mathbf{r}_i), \tag{2}$$

with $\mathbf{R}_a$ being the Cartesian coordinates of QM atom a, and $v(\mathbf{x})$ is the ESP produced by the MM molecules, namely

$$v(\mathbf{x}) = \sum_j^{\text{MM}} \frac{q_j}{|\mathbf{x} - \mathbf{r}_j|}. \tag{3}$$

The ES interaction energy between the QM and MM molecules can be written as

$$E_{\text{int}} = \int d\mathbf{x}\rho(\mathbf{x})v(\mathbf{x}), \tag{4}$$

where $\rho(\mathbf{x}) = \langle\Psi|\hat{\rho}(\mathbf{x})|\Psi\rangle$. In the point charge approximation, the above E_{int} is approximated as

$$E_{\text{int}} \simeq \sum_a Q_a V_a, \tag{5}$$

where Q_a is the ESP derived partial charge, and V_a is the ESP of the MM molecules acting on the QM atom a, i.e. $V_a = v(\mathbf{R}_a)$. We now utilize the fact that Q_a can be expressed as $Q_a = \langle\Psi|\hat{Q}_a|\Psi\rangle$ [6–9], where $\hat{Q}_a$ is the ESP derived partial charge operator. The corresponding Schrödinger equation may be written as

$$[\hat{H}_0 + \sum_a \hat{Q}_a V_a]|\Psi\rangle = \mathcal{E}|\Psi\rangle. \tag{6}$$

The above equation can be obtained by approximating the charge density operator $\hat{\rho}(\mathbf{x})$ as

$$\hat{\rho}(\mathbf{x}) \simeq \hat{\rho}_{pc}(\mathbf{x}) \equiv \sum_a \hat{Q}_a \delta(\mathbf{x} - \mathbf{R}_a), \tag{7}$$

where "pc" stands for the point charge approximation. By separating the nuclear and electronic contributions of $\hat{Q}_a$ such that $\hat{Q}_a = Z_a + \hat{Q}_a^{(\mathrm{e})}$, we have

$$\hat{\rho}_{pc}(\mathbf{x}) = \sum_a Z_a \delta(\mathbf{x} - \mathbf{R}_a) + \sum_a \hat{Q}_a^{(\mathrm{e})} \delta(\mathbf{x} - \mathbf{R}_a). \tag{8}$$

The above approximation states that the electron distribution is localized at the QM nuclei, which is, however, not the case for real molecules. To account for the finite extent of electron distribution, we modify Eq. (8) as follows:

$$\hat{\rho}_{sc}(\mathbf{x}) = \sum_a Z_a \delta(\mathbf{x} - \mathbf{R}_a) + \sum_a \hat{Q}_a^{(\mathrm{e})} F_a(\mathbf{x}), \tag{9}$$

where $F_a(\mathbf{x})$ is some normalized distribution function. We refer to the above $\rho_{sc}(\mathbf{x})$ as the screened charge (sc) approximation to $\rho(\mathbf{x})$. Furthermore, we decompose $F_a(\mathbf{x})$ into the contribution of core and valence electrons, such that

$$F_a(\mathbf{x}) = \kappa_a \delta(\mathbf{x} - \mathbf{R}_a) + (1 - \kappa_a) F_a^{val}(\mathbf{x}), \tag{10}$$

where κ_a is a parameter specifying the ratio of core electrons over all electrons in atom a, and $F_a^{val}(\mathbf{x})$ is a normalized function that accounts for the finite extent of valence electrons. Note that the distribution of core electrons is approximated by the delta function, and that in the limit $\kappa_a \to 1$ the screened charge operator $\hat{\rho}_{sc}(\mathbf{x})$ reverts to the point charge operator $\hat{\rho}_{pc}(\mathbf{x})$. In this paper we employ a Slater-type function for $F_a^{val}(\mathbf{x})$, that is,

$$F_a^{val}(\mathbf{x}) = \frac{\zeta_a^3}{8\pi} e^{-\zeta_a |\mathbf{x} - \mathbf{R}_a|}, \tag{11}$$

where the exponent ζ_a is determined by a least-squares fit to ab initio ESP (see Sec. III). We also tested several different forms of F_a^{val} such as $r^{2n-2}\exp(-\zeta_a r)$ and $\exp(-\zeta_a r)/r$, and find that they give similar numerical performance. On the other hand, the Gaussian-type function, $\exp(-\zeta_a r^2)$, was found to be less accurate in reproducing the ESP of the QM molecule. This is probably because the tail part of charge distribution decays too rapidly with the single Gaussian approximation. With the $\hat{\rho}_{sc}(\mathbf{x})$ defined above, we consider an approximate Schrödinger equation of the form

$$[\hat{H}_0 + \int d\mathbf{x} \hat{\rho}_{sc}(\mathbf{x}) v(\mathbf{x})] |\Psi\rangle = \mathcal{E} |\Psi\rangle. \tag{12}$$

Now utilizing the relation

$$\int d\mathbf{x} F_a^{val}(\mathbf{x}) \frac{1}{|\mathbf{x}-\mathbf{r}_j|} = \frac{1}{R_{aj}} - \frac{(1+\zeta_a R_{aj}/2)e^{-\zeta_a R_{aj}}}{R_{aj}} \tag{13}$$

with $R_{aj} = |\mathbf{R}_a - \mathbf{r}_j|$, and substituting Eq. (9) into Eq. (12), we obtain

$$[\hat{H}_0 + \sum_a (Z_a V_a + \hat{Q}_a^{(\mathrm{e})} V_a^{(\mathrm{e})})]|\Psi\rangle = \mathcal{E}|\Psi\rangle. \tag{14}$$

where V_a and $V_a^{(\mathrm{e})}$ are defined by

$$V_a = \sum_j^{\mathrm{MM}} \frac{q_j}{R_{aj}}, \tag{15}$$

and

$$V_a^{(\mathrm{e})} = \sum_j^{\mathrm{MM}} \frac{q_j}{R_{aj}} - (1-\kappa_a) \sum_j^{\mathrm{MM}} q_j \frac{(1+\zeta_a R_{aj}/2)e^{-\zeta_a R_{aj}}}{R_{aj}}. \tag{16}$$

Note that the second term in Eq. (16) describes the penetration effects of valence electrons. The above equation can be written more concisely as

$$V_a^{(\mathrm{e})} = \sum_j^{\mathrm{MM}} \frac{q_j}{R_{aj}} f_{aj}, \tag{17}$$

where f_{aj} represents a damping factor given by

$$f_{aj} = 1 - (1-\kappa_a)(1+\zeta_a R_{aj}/2)e^{-\zeta_a R_{aj}}, \tag{18}$$

which satisfies $0 < f_{aj} < 1$.

We emphasize that in the above screened charge model the QM nuclei are still represented by point charges. The damping function affects only the ES interaction between QM (valence) electrons and MM point charges, unlike traditional polarizable models in which a damping function is applied to the overall atomic charge (for example, see [6]). As such, we expect that the present approach gives a more faithful representation of molecular interactions, which, in turn, facilitates ab initio determination of the damping parameter ζ_a (see Sec. IV). Before proceeding, we note that the ESP of the QM molecule is given by

$$\varphi(\mathbf{r}) = \int d\mathbf{x} \frac{\langle\Psi|\hat{\rho}_{sc}(\mathbf{x})|\Psi\rangle}{|\mathbf{r}-\mathbf{x}|} \tag{19}$$

$$= \sum_a^{\mathrm{QM}} \frac{Q_a}{|\mathbf{r}-\mathbf{R}_i|} - \sum_a^{\mathrm{QM}} (1-\kappa_a) Q_a^{(\mathrm{e})} \frac{(1+\zeta_a|\mathbf{r}-\mathbf{R}_a|/2)e^{-\zeta_a|\mathbf{r}-\mathbf{R}_a|}}{|\mathbf{r}-\mathbf{R}_a|}, \tag{20}$$

where Q_a is the (unscreened) ESP charge given by $Q_a = \langle\Psi|\hat{Q}_a|\Psi\rangle$, and $Q_a^{(\mathrm{e})}$ is the electronic part of partial charge, namely $Q_a^{(\mathrm{e})} = \langle\Psi|\hat{Q}_a^{(\mathrm{e})}|\Psi\rangle = Q_a - Z_a$.

III. COMPUTATIONAL DETAILS

As a numerical test, we performed a series of QM/MM calculations of a solute molecule dissolved in 252 water molecules. Here we described the solute molecule with the HF/6-31+G(d,p) method (unless otherwise noted) and the solvent with the TIP3P model. During the QM/MM calculation, the solute geometry was fixed to that obtained from the geometry optimization at the B3LYP/6-31+G(d,p)/PCM level.

For the sake of comparison, we performed three types of QM/MM calculations: First, as a reference, we performed a direct QM/MM MD calculation for 240 ps, in which the Schrödinger equation in Eq. (1) was solved at each MD step. In the direct QM/MM calculation, the MM point charges were inserted directly into the Fock matrix of the QM Hamiltonian, and hence penetration effects of the QM molecule are rigorously included. Second, we performed a mean-field (MF) QM/MM calculation [12–14] based on Eq. (6). Specifically, we solve the following equation for the QM molecule

$$[\hat{H}_0 + \sum_a \hat{Q}_a \langle V_a \rangle] |\tilde{\Psi}\rangle = \mathcal{E} |\tilde{\Psi}\rangle, \tag{21}$$

where $\langle V_a \rangle$ is the statistical average of the solvent potential. The latter is obtained from a classical MD sampling of solvent for 600 ps. The QM calculation of $\tilde{\Psi}$ and the MD sampling of solvent are iterated until self-consistency is achieved. The MF-QM/MM method is analogous to traditional solvation models (e.g. the PCM and RISM-SCF methods) in that the mean solvent potential is included in the QM Hamiltonian. The essential difference is that we sample the solvent configurations explicitly via MD calculation. When compared to the direct QM/MM calculation, the MF-QM/MM method has the advantage that it can reduce the number of QM calculations significantly (typically on the order of 10–100), while allowing an extensive sampling of the MM environment [12–14]. Third, we performed a similar MF-QM/MM calculation based on the screened charge model. Here, we solve the following equation

$$[\hat{H}_0 + \sum_a (Z_a \langle V_a \rangle + \hat{Q}_a^{(\mathrm{e})} \langle V_a^{(\mathrm{e})} \rangle)] |\tilde{\Psi}\rangle = \mathcal{E} |\tilde{\Psi}\rangle, \tag{22}$$

where $\langle V_a \rangle$ and $\langle V_a^{(\mathrm{e})} \rangle$ are, respectively, statistical average of V_a and $V_a^{(\mathrm{e})}$ defined by Eqs. (15) and (16). Note that $V_a^{(\mathrm{e})}$ accounts for charge penetration effects of the QM molecule via the damping factor in Eq. (18). Other computational details are the same as those of the MF-QM/MM calculation based on Eq. (21).

The screened charge operator in Eq. (9) has two adjustable parameters. One is the ratio of core electrons over all electrons κ_a, and the other is the exponent of the Slater-type function ζ_a. In this paper we determine the former as $\kappa_a = Q_a^{\rm core}/Q_a^{\rm ref}$, where $Q_a^{\rm core}$ and $Q_a^{\rm ref}$ denote the charge of core and all electrons of atom a, respectively. The $Q_a^{\rm core}$ is chosen as 0 for a hydrogen atom, $-2e$ for carbon and oxygen atoms, and $-10e$ for phosphate and chloride atoms. The $Q_a^{\rm ref}$ is determined as $Q_a^{\rm ref} = \langle \Psi^{\rm ref} | \hat{Q}_a^{\rm (e)} | \Psi^{\rm ref} \rangle$, where $\Psi^{\rm ref}$ is some reference wavefunction. In this paper, we choose the latter as $\Psi^{\rm ref} \equiv \tilde{\Psi}$, where $\tilde{\Psi}$ is obtained from the MF-QM/MM calculation. Next, we determine the exponent of the Slater-type function ζ_a as follows: First, we calculate the usual ESP charge as $Q_a = \langle \tilde{\Psi} | \hat{Q}_a | \tilde{\Psi} \rangle$ by using the Spackman scheme [25]. In the latter calculation, the grid points are placed on fused vdW spheres with a scaling factor of $1.4, 1.5, \ldots, 2.6$. Next, we determine the parameter ζ_a by fitting $\varphi(\mathbf{x})$ in Eq. (20) to ab initio ESP of the QM molecule. Specifically, we minimize the following objective function

$$\chi^2(\{\zeta_a\}) = \frac{1}{N_{grid}} \sum_{k=1}^{N_{grid}} \left(\varphi^{ai}(\mathbf{x}_k) - \varphi(\mathbf{x}_k) \right)^2, \tag{23}$$

where $\varphi^{ai}(\mathbf{x}_k)$ is the value of ab initio ESP derived from $\tilde{\Psi}$, i.e.

$$\varphi^{ai}(\mathbf{x}_k) = \int d\mathbf{x} \frac{\langle \tilde{\Psi} | \hat{\rho}(\mathbf{x}) | \tilde{\Psi} \rangle}{|\mathbf{x}_k - \mathbf{x}|}, \tag{24}$$

and $\{\mathbf{x}_k\}$ are grid points placed on fused vdW spheres with a scaling factor of $1.00, 1.05, \ldots, 2.5$. Note that the grid points are placed in both the inner and outer regions of the QM molecule (separated by a scaling factor of 1.4). This is essential for including penetration effects at short range while retaining the accuracy of ESP at long range. The minimization of χ^2 in Eq. (23) was performed as a function of $\{\zeta_a\}$ with the downhill simplex method. It should be noted that the above optimization may yield unphysical values of ζ_a if the QM molecule has buried atoms. If that case, it may be a good idea to add some penalty term to the objective function, e.g. $\lambda \sum_a (\zeta_a - \zeta_a^0)^2$, where λ is a restraint parameter and $\{\zeta_a^0\}$ are some reference values. For simple molecules studied below, we find that the optimization proceeds successfully without such a penalty term. The vdW radii used in this paper are taken from Gavezzotti [26] and Spackman [27] and are listed Table I.

Before proceeding, we emphasize that the procedure described above does not aim at obtaining a common (or universal) set of exponential parameters $\{\xi_a\}$ for use in general MM

force fields. Rather, we calculate the exponent specifically for each QM molecule, on the same footing as the ESP charge itself. We expect that this procedure is reasonable because the exponent should in principle depend on the polarization of the QM wave function in a specific environment as well as the net charge of the QM molecule.

IV. RESULTS AND DISCUSSION

We first display in Fig. 1 the radial distribution functions (RDFs) calculated for a QM water molecule in TIP3P water. This figure shows the results obtained from (i) the direct QM/MM calculation, (ii) MF-QM/MM calculation based on the point charge approximation (labeled as "MF-QM/MM(pc)"), and (iii) MF-QM/MM calculation based on the screened charge approximation (labeled as "MF-QM/MM(sc)"). Fig. 1 shows that the MF-QM/MM(pc) method slightly overestimates the height of the first peak as compared to the direct QM/MM calculation, while the screened MF-QM/MM method gives more accurate peak heights. This indicates that charge penetration effects are present even for this neutral molecule and they are appropriately taken into account by the screened charge model. We also note that the present calculation somewhat overestimates the height of the first peak as compared to experiment (2.8 for O-OW RDF and 1.2 for O-HW RDF [28]). This is partly because of the present use of HF method for the QM molecule, which tends to overpolarize the QM wave function, and partly because of the use of TIP3P model for water molecules (see Sec. V).

Penetration effects become stronger for negatively charged ions. Fig. 2 displays the RDF obtained for the chloride ion (Cl^-) in water. As seen, there is a clear discrepancy between the direct QM/MM and MF-QM/MM(pc) results, while the discrepancy is almost eliminated in the screened MF-QM/MM calculation. To obtain more insight, we depict in Fig. 2 (c) the ESP generated by the chloride ion. This figure shows that the ESP calculated with a point charge (labeled as "pc") deviates considerably from the ab initio ESP (labeled as "QM") at short distances ($r < 2.4$ Å). Note that the latter distance is within 1.4 times the vdW radius of the chloride atom (which equals 2.5 Å, see Table I), and that the standard ESP fitting protocol [27] spans the ESP grid for $r \geq 2.5$ Å. Since the first peak of Cl-HW RDF appears at $r \sim 2.4$ Å, it is affected by the insufficient accuracy of the (raw) ESP charge operator at short range. On the other hand, the screened ESP function $\varphi(\mathbf{x})$ in Eq. (20) (labeled

as "sc") almost coincides with the ab initio ESP in the entire region, and as a result the obtained RDF is in much better agreement with the direct QM/MM calculation.

The discrepancy between the direct and MF-QM/MM(pc) results becomes more significant for different anions. Fig. 3 displays the RDF obtained for a hydroxide ion (OH^-) in water. A previous study suggests that the point charge approximation is not sufficiently accurate for modeling the hydroxide ion in water [29]. Indeed, Fig. 3 reveals that the discrepancy between the direct and MF-QM/MM(pc) results is substantial. Nevertheless, we see that the discrepancy is almost eliminated by the screened charge model, which demonstrates the importance of charge penetration effects for the hydroxide ion. Fig. 4 illustrates the ESP contour map of the OH^- ion. As seen, the ESP obtained from the screened charges agrees very well with that obtained from continuous charge density, while the ESP obtained from point charge approximation exhibits noticeable difference at short distances. It is also interesting that the ESP obtained from the charge density shows local anisotropy in the vicinity of the O atom by reflecting the lone electron pairs. On the other hand, the local anisotropy is not observed for the screened charge model, because the latter approximates the charge density as the sum of atom-centered spherical ones.

The situation becomes quite different for a positively charged ion. Fig. 5 depicts the RDF obtained for a sodium ion (Na^+) in water. Note that with the present computational protocol, all the electrons of Na^+ are counted as core electrons, hence $Q_a^{\mathrm{core}} = -10e$ and $\kappa_a = 1$. This means that the screened charge model becomes identical to the point charge model for the sodium ion. Therefore, to account for the penetration effects of outer electrons, we counted only the two $1s$ electrons as "core" electrons and the remaining as "valence" electrons. Fig. 5 (a) depicts the RDF thus obtained, which reveals that all the three QM/MM methods give essentially the same results. This observation is also consistent with the ESP of the sodium ion shown in Fig. 5 (b). The above result suggests that charge penetration effects of the sodium ion are much smaller than those for the other ions because of a more localized charge distribution.

Finally, we consider the phosphate ion (PO_4^{3-}) as an example of highly charged solute. Fig. 6 displays the RDF calculated at the HF/6-31+G(d) level. As expected, the MF-QM/MM(pc) method gives more structured RDFs than the direct QM/MM calculation due to the overestimated ES interactions at short range. On the other hand, the screened MF-QM/MM method gives better agreement with the direct one. A closer inspection of Fig. 6

reveals that the agreement of the direct and MF-QM/MM(sc) results is slightly worse than for the other ions (e.g., Cl^-), which may be because the solute-solvent interactions are much stronger for the $PO_4{}^{3-}$ ion. Table II compares the calculated results with experimental ones [30]. Here, we re-calculated all the MF-QM/MM results at the B3LYP/aug-cc-pVTZ level to obtain more reliable data. Table II shows that the screened MF-QM/MM method gives better agreement with experiment than the MF-QM/MM(pc) method, particularly for the first peak of RDFs. In addition, we list in Table II the results of the RISM-SCF-SEDD method [24] calculated for the same system at the B3LYP level. Comparison with the latter method shows that the screened MF-QM/MM calculation gives similar results for this ion. Based on the above observations, we expect that the screened charge model in Eq. (9) gives a reasonably accurate description of solvated ions in aqueous solution.

V. CONCLUDING REMARKS

In this paper we have explored a way to improve the ESP derived partial charge operator for including penetration effects at short range. To do so, we modeled the charge distribution of valence electrons with a Slater-type function, $F^{val}(\mathbf{x})$, and determined the necessary parameters from ab initio ESP calculation. We applied the obtained model to several ions in solution and demonstrated its accuracy by comparison with a direct QM/MM calculation. The main benefit of the present approach (rather than using the exact charge density in Eq. (2)) is that one can recast the QM-MM interactions into the form of an interaction site model. This should facilitate the combined use of the screened charge operator with other classical theories for the environment (e.g., 1D- and 3D-RISM methods [10]).

There are three additional points to be mentioned. First, as observed in Sec. IV, the (raw) ESP charge operator overestimates short-range ES interactions, the degree of which depends on the type of solute and solvent. We expect that the degree of overestimation is greater for systems with solute-solvent hydrogen bonds (e.g., ionic systems in aqueous solution), while it is smaller for systems in polar aprotic solvents (e.g., acetonitrile). Second, although we have based our discussion on the distributed monopole model, one may utilize a distributed multipole model for enhanced accuracy [20]. For this purpose, a screening procedure similar to Eq. (9) may be useful in properly attenuating the ES interactions at short range. Third, since the TIP3P model is based on a point charge model, the solute-

solvent ES interactions may also be overestimated by the TIP3P model. In that case, it may be advantageous to employ some Gaussian or Slater charge model for water [1–5] rather using the TIP3P model. An interesting problem here is to combine the screened charge operator for the solute with a Gaussian or Slater charge model for water. The benefit of this approach is that QM/MM interactions can be written in a pairwise analytical form, which may facilitate the implementation of MD simulation. Exploring those problems remains the subject of future study.

Acknowledgments

This work was supported by the Grant-in-Aid for Scientific Research (21350010) and that on Innovative Areas (21118508) from the Ministry of Education, Culture, Sports, Science and Technology (MEXT) of Japan.

[1] M. A. Freitag, M. S. Gordon, J. H. Jensen, and W. J. Stevens, J. Chem. Phys. **112**, 7300 (2000).

[2] G. A. Cisneros, S. N. Tholander, O. Parisel, T. A. Darden, D. Elking, L. Perera, and J. P. Piquemal, Int. J. Quantum Chem. **108**, 1905 (2008).

[3] L. V. Slipchenko and M. S. Gordon, Mol. Phys. **107**, 999 (2009).

[4] B. Wang and D. G. Truhlar, J. Chem. Theory Comput. **6**, 3330 (2010).

[5] A. S. Werneck, T. M. R. Filho, and L. E. Dardenne, J. Phys. Chem. A **112**, 268 (2008).

[6] A. Morita and S. Kato, J. Chem. Phys. **108**, 6809 (1998).

[7] A. Morita and S. Kato, J. Am. Chem. Soc. **119**, 4021 (1997).

[8] S. Ten-no, F. Hirata, and S. Kato, J. Chem. Phys. **100**, 7443 (1994).

[9] H. Sato, F. Hirata, and S. Kato, J. Chem. Phys. **105**, 1546 (1996).

[10] F. Hirata, ed., *Molecular Theory of Solvation* (Kluwer, New York, 2004).

[11] H. Nakano, T. Yamamoto, and S. Kato, J. Chem. Phys. **132**, 044106 (2010).

[12] T. Yamamoto, J. Chem. Phys. **129**, 244104 (2008).

[13] H. Nakano and T. Yamamoto, J. Chem. Phys. **136**, 134107 (2012).

[14] T. Kosugi and S. Hayashi, J. Chem. Theory Comput. **8**, 322 (2012).

[15] M. Higashi and D. G. Truhlar, J. Chem. Theory Comput. **4**, 790 (2008).

[16] M. Higashi and D. G. Truhlar, J. Chem. Theory Comput. **4**, 1032 (2008).

[17] S. Hayashi and I. Ohmine, J. Phys. Chem. B **104**, 10678 (2000).

[18] S. Aono, T. Yamamoto, and S. Kato, J. Chem. Phys. **134**, 144108 (2011).

[19] T. Yamamoto and S. Kato, J. Chem. Phys. **126**, 224514 (2007).

[20] N. Ferre and J. G. Angyan, Chem. Phys. Lett. **356**, 331 (2002).

[21] C. Houriez, N. Ferre, M. Masella, and D. Siri, J. Chem. Phys. **128**, 244504 (2008).

[22] F. Aquilante, L. De Vico, N. Ferre, G. Ghigo, P.-A. Malmqvist, P. Neogrady, T. B. Pedersen, M. Pitonak, M. Reiher, B. O. Roos, et al., J. Comp. Chem. **31**, 224 (2010).

[23] I. Navizet, Y.-J. Liu, N. Ferre, H.-Y. Xiao, W.-H. Fang, and R. Lindh, J. Am. Chem. Soc. **132**, 706 (2010).

[24] D. Yokogawa, H. Sato, and S. Sakaki, J. Chem. Phys. **126**, 244504 (2007).

[25] M. A. Spackman, J. Comput. Chem. **17**, 1 (1996).

[26] A. Gavezzotti, J. Am. Chem. Soc. **105**, 5220 (1983).

[27] M. A. Spackman, J. Chem. Phys. **85**, 6579 (1986).

[28] A. K. Soper, Chem. Phys. **258**, 121 (2000).

[29] H. Takahashi, H. Ohno, T. Yamauchi, R. Kishi, S. Furukawa, M. Nakano, and N. Matubayasi, J. Chem. Phys. **128**, 064507 (2008).

[30] P. E. Mason, J. M. Cruickshank, G. W. Neilson, and P. Buchanan, Phys. Chem. Chem. Phys. **5**, 4686 (2003).

TABLE I: Van der Waals (vdW) radii (in Å) taken from Gavezzotti and Spackman [26, 27].

H	C	N	O	Na	P	Cl
1.20	1.50	1.50	1.40	1.80	1.96	1.80

TABLE II: Position of the first peak of solute-solvent RDF for the phosphate ion (PO_4^{3-}) in aqueous solution. MF-QM/MM(pc) and MF-QM/MM(sc) refer to the mean-field QM/MM calculation with point charge and screened charge approximations, respectively. The QM calculation is performed at the B3LYP/aug-cc-pVTZ level. For comparison, the results of the RISM-SCF-SEDD method [24] and the experiment results obtained by Mason et al. [30] are shown. C.N. stands for the coordination number.

	MF-QM/MM(pc)	MF-QM/MM(sc)	RISM-SCF-SEDD	Expt.
r(P-OW) (Å)	3.53	3.78	3.67	3.7
r(O-HW) (Å)	1.58	1.83	1.69	1.8
C.N.(P-OW)	16.2	16.5	18.4	15±3
C.N.(O-HW)	4.0	4.1	5.2	3

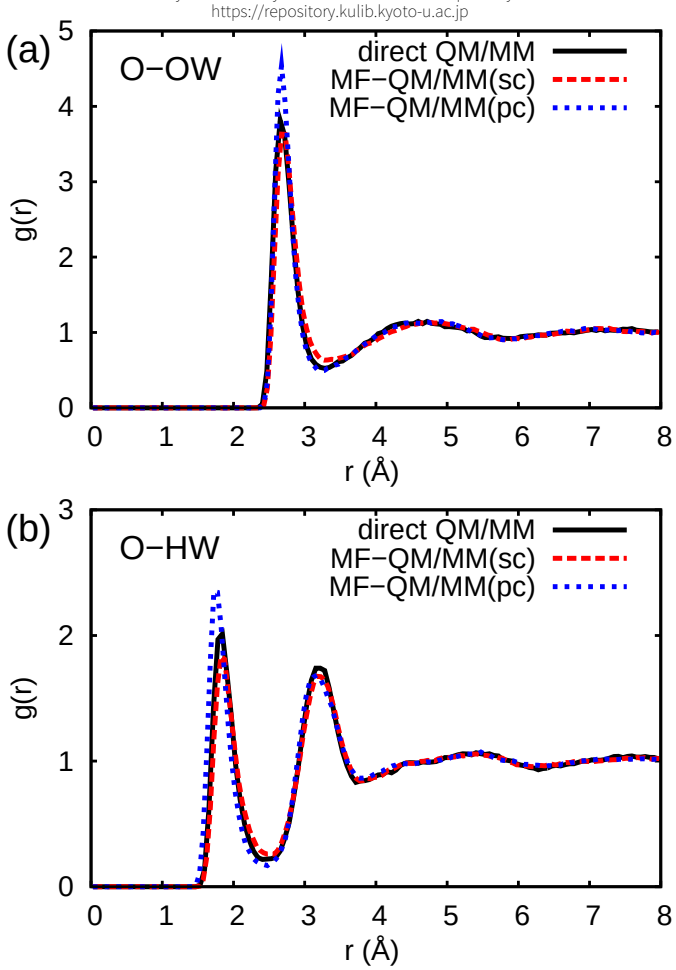

FIG. 1: Radial distribution functions (RDFs) of solvent water molecules around a QM water molecule obtained from QM/MM calculations. The direct QM/MM result is compared with the mean-field (MF) QM/MM results obtained with the point charge (pc) or screened charge (sc) approximation. The QM molecule is described with the HF/6-31+G(d,p) method while the solvent with the TIP3P model.

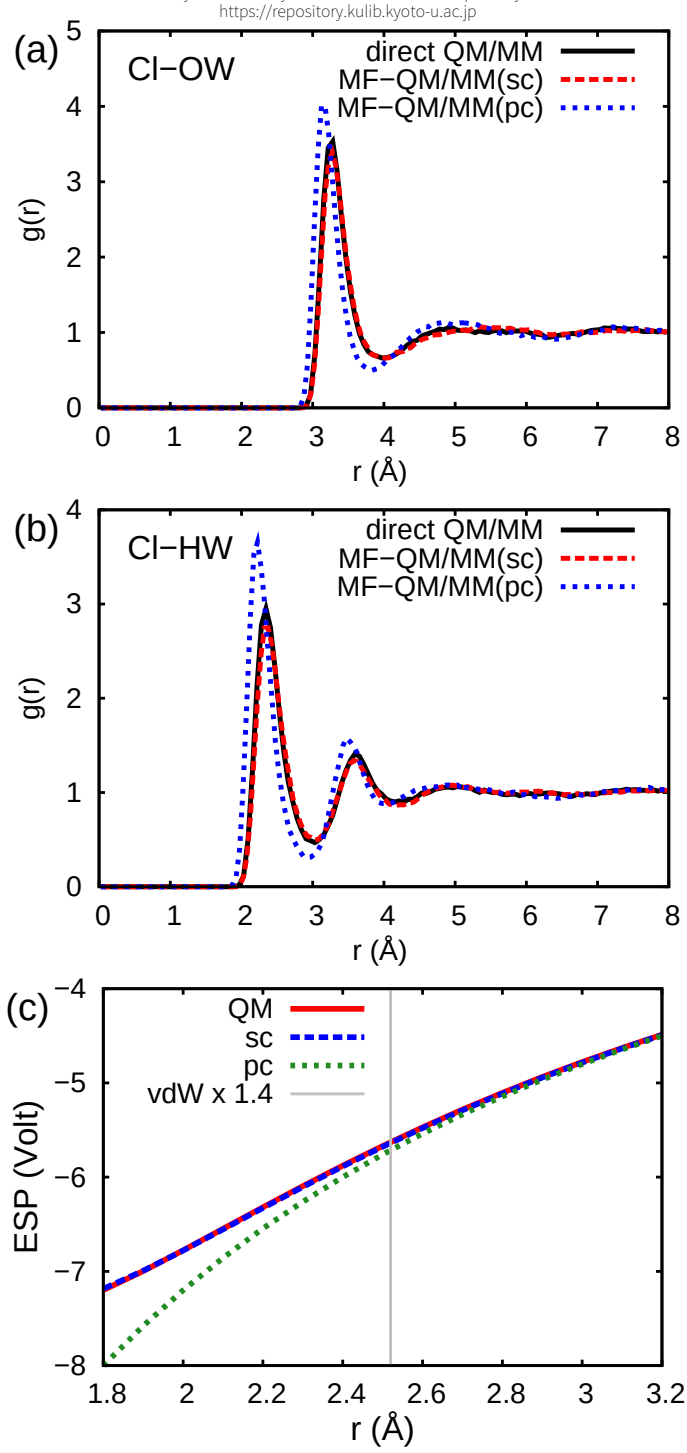

FIG. 2: RDFs of solvent water molecules around the chloride ion (Cl^-) obtained from QM/MM calculations. Panel (c) depicts the electrostatic potential (ESP) of the chloride ion calculated with several different methods (see the main text). The vertical line in panel (c) indicates 1.4 times the vdW radius of the chloride atom (see Table I).

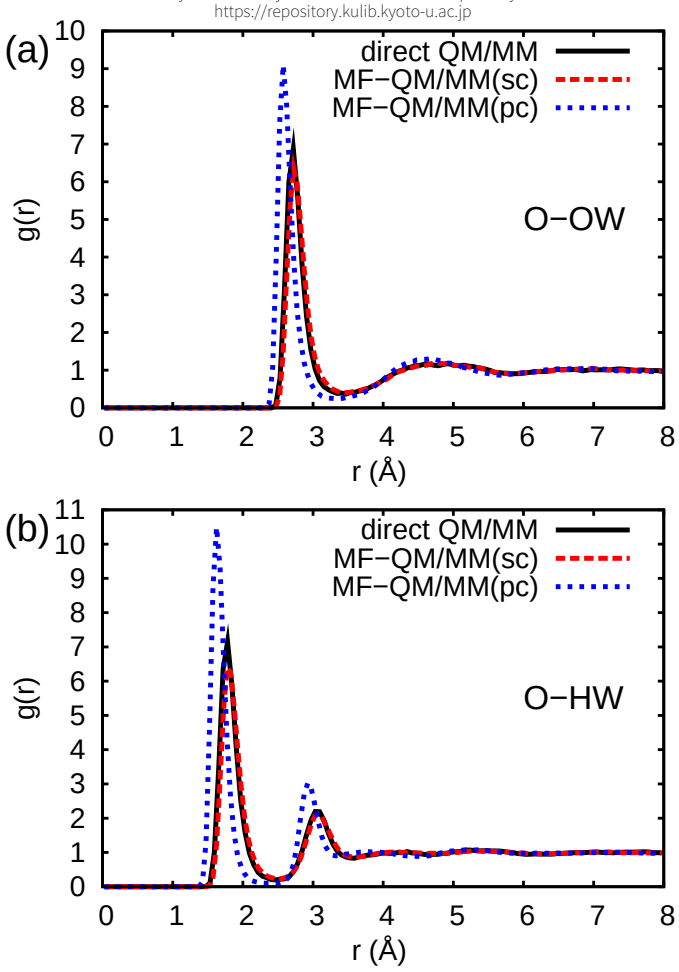

FIG. 3: RDFs of solvent water molecules around a hydroxide ion (OH^-).

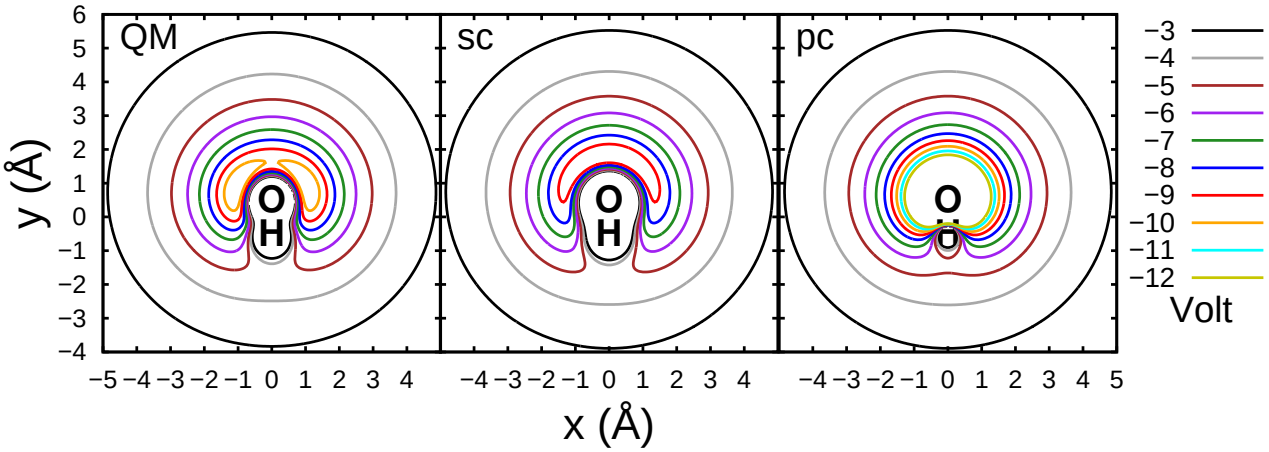

FIG. 4: ESP contour map of the hydroxide ion (OH^-). The QM molecule is represented by (a) continuous charge density, (b) screened charges placed on the O and H atoms, and (c) ESP point charges placed on the O and H atoms.

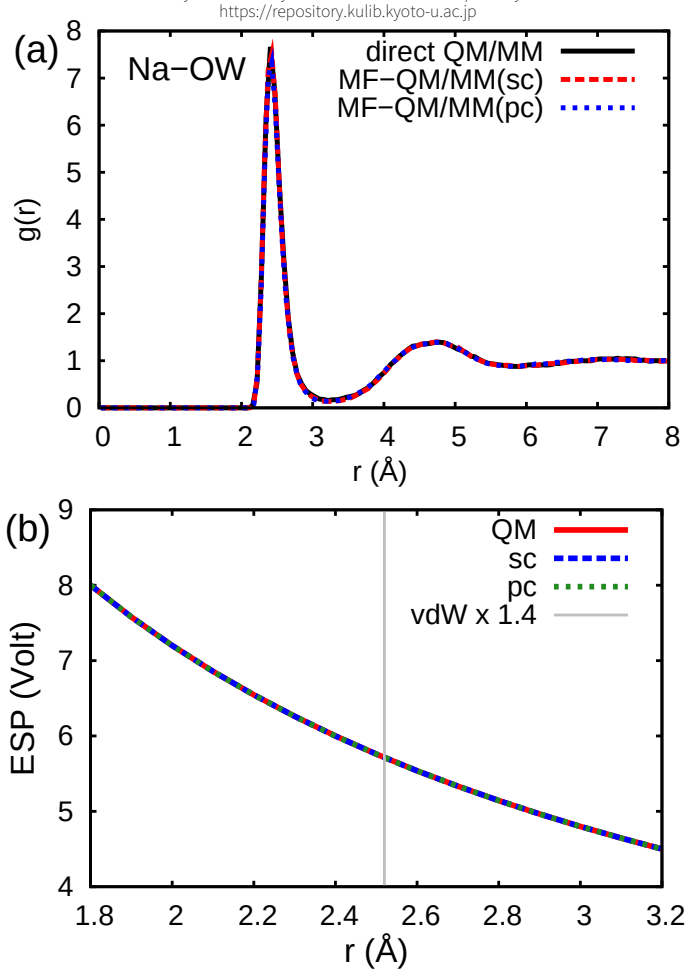

FIG. 5: RDF of solvent water molecules around a sodium ion (Na^+). Panel (b) displays the electrostatic potential (ESP) produced by the sodium ion. The vertical line in panel (b) indicates 1.4 times the vdW radius of the sodium atom (see Table I).

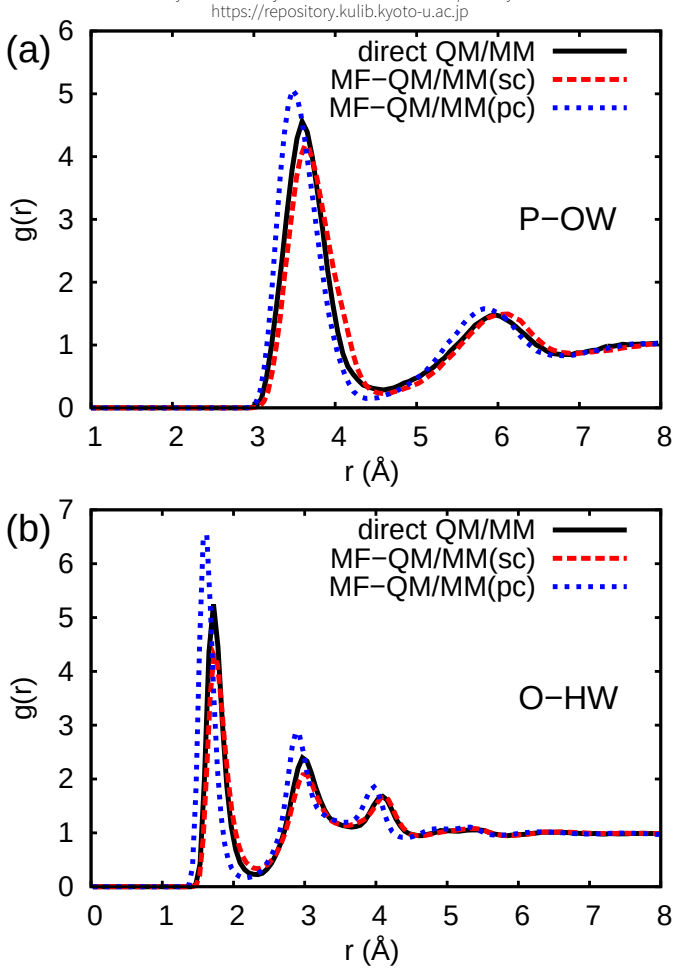

FIG. 6: RDFs of solvent water molecules around a phosphate ion (PO_4^{3-}).